Monte Carlo verification of IMRT dose distributions from a commercial treatment planning optimization system

2000 Phys. Med. Biol. 45 2483

(http://iopscience.iop.org/0031-9155/45/9/303)

Phys. Med. Biol. **45** (2000) 2483–2495. Printed in the UK PII: S0031-9155(00)12146-3

Monte Carlo verification of IMRT dose distributions from a commercial treatment planning optimization system

C-M Ma, T Pawlicki, S B Jiang, J S Li, J Deng, E Mok, A Kapur, L Xing, L Ma and A L Boyer

Radiation Oncology Department, Stanford University School of Medicine, Stanford, CA 94305, USA

E-mail: cma@reyes.stanford.edu

Received 25 February 2000, in final form 8 May 2000

Abstract. The purpose of this work was to use Monte Carlo simulations to verify the accuracy of the dose distributions from a commercial treatment planning optimization system (Corvus, Nomos Corp., Sewickley, PA) for intensity-modulated radiotherapy (IMRT). A Monte Carlo treatment planning system has been implemented clinically to improve and verify the accuracy of radiotherapy dose calculations. Further modifications to the system were made to compute the dose in a patient for multiple fixed-gantry IMRT fields. The dose distributions in the experimental phantoms and in the patients were calculated and used to verify the optimized treatment plans generated by the Corvus system. The Monte Carlo calculated IMRT dose distributions agreed with the measurements to within 2% of the maximum dose for all the beam energies and field sizes for both the homogeneous and heterogeneous phantoms. The dose distributions predicted by the Corvus system, which employs a finite-size pencil beam (FSPB) algorithm, agreed with the Monte Carlo simulations and measurements to within 4% in a cylindrical water phantom with various hypothetical target shapes. Discrepancies of more than 5% (relative to the prescribed target dose) in the target region and over 20% in the critical structures were found in some IMRT patient calculations. The FSPB algorithm as implemented in the Corvus system is adequate for homogeneous phantoms (such as prostate) but may result in significant under- or over-estimation of the dose in some cases involving heterogeneities such as the air–tissue, lung–tissue and tissue–bone interfaces.

(Some figures in this article are in colour only in the electronic version; see www.iop.org)

1. Introduction

For the last few years, extensive research has been carried out to develop conformal radiotherapy using computer-controlled linear accelerators equipped with multileaf collimators (MLC) (Boesecke *et al* 1988, Leibel *et al* 1992, LoSasso *et al* 1993, Powlis *et al* 1993, Mageras *et al* 1994, Brewster *et al* 1995, Fraass *et al* 1995, McShan *et al* 1995, Yu *et al* 1995). More recently, intensity modulated radiotherapy (IMRT) has been developed (Brahme 1988, Convery and Rosenbloom 1992, Webb 1992, Boyer *et al* 1997) and implemented (Ling *et al* 1996, Boyer *et al* 1998) that uses computer-controlled modulation of x-ray fields by the MLC. It is anticipated that conformal radiotherapy will provide radiation oncologists with a significantly improved tool to deliver high doses of ionizing radiation to some tumour sites while reducing doses to adjacent normal tissue below levels to which they are unavoidably exposed by currently available techniques. Thus, acute and chronic toxicity associated with treatment of a tumour volume by radiation may be significantly reduced or delayed for certain sites of malignant presentations.

0031-9155/00/092483+13$30.00

The use of conformal radiotherapy, especially with the IMRT technique, is a major departure from the way radiotherapy is currently delivered. Although the use of MLCs provides the possibility of achieving better dose distributions conformed to tumour targets, it also increases the complexity of treatment. The sequences of leaf movement and their associated effects on the dose delivered to the patient may vary significantly depending on the accelerator and the MLC design. Important factors include the variation of the accelerator head scatter component in the MLC-collimated beam (Convery and Webb 1997), the amount of photon leakage through the leaves (Wang *et al* 1996, Webb 1997, Holmes *et al* 1997), the scatter from the leaf ends, the 'tongue and groove' effect (Chui *et al* 1994, Wang *et al* 1996), the effect of back-scattered photons from the moving jaws and MLC leaves on the monitor chamber signal (Hounsell 1998). Traditionally, patient dose calculations in radiotherapy have been based on correcting measured dose distributions. New dose calculation algorithms have been developed to predict the patient dose from 'first principles' using a model of radiation transport (Mackie *et al* 1995). Comparisons of the traditional photon algorithms and the newer ones have been reviewed by Wong and Purdy (1990), Cunningham and Battista (1995) and Mackie *et al* (1996). Due to the lack of electron transport, the conventional dose calculation algorithms often failed to predict the dose distribution accurately near inhomogeneities (Mackie *et al* 1996, Mohan 1997, DeMarco *et al* 1998, Wang *et al* 1998, Ma *et al* 1999). Furthermore, the inverse-planning algorithms for beam optimization have all used approximations to speed up the dose computation that may introduce significant uncertainty in the calculated dose distributions, especially in the presence of heterogeneities. When simple source models are used in the dose computation, the correlation between the calibrated reference dose and the dose related to a beam segment may be lost. All the above imply a potential problem with the prediction of the dose distributions in a patient for an IMRT treatment.

Oldham and Webb (1997) reported differences in excess of 10% in the absolute dose between the optimization dose calculations and measurements (using film) of fields delivered by a dynamic MLC. The differences were attributed partially to the nonlinearity of dose per monitor unit (MU) for small MU deliveries (the actual dose delivered per MU increased by more than 10% from MU = 20 to MU = 1). Wang *et al* (1996) reported that for the Memorial Hospital's dynamic MLC delivery process, the discrepancies between the calculated dose and the measured dose were in excess of 5% if various effects related to the MLC construction, such as accelerator head scatter, were not properly accounted for. The uncertainty in the doses calculated by a conventional dose calculation algorithm was 5–10% in the presence of heterogeneities (Mohan 1997). Our recent Monte Carlo results were consistent with these findings (Ma *et al* 1999).

The purpose of this work was to verify the accuracy of the IMRT dose distributions from a commercial treatment planning optimization system (Corvus, Nomos Corp., Sewickley, PA) using Monte Carlo simulations. We have used the EGS4/BEAM Monte Carlo code system (Nelson *et al* 1985, Rogers *et al* 1995a, b) to simulate the clinical photon beams from two linear accelerators, Varian Clinac 2100C and 2300C/D (Varian Oncology, Palo Alto, CA). The EGS4/DOSXYZ code (Rogers *et al* 1995a, Ma *et al* 1995) was modified to compute the dose in a patient (a three-dimensional phantom built from the CT data) for multiple fixed-gantry fields. Phantom measurements were performed to commission the Monte Carlo system. The dose distributions in the experimental phantoms and in the patients were calculated and used to verify the optimized treatment plans generated by the Corvus inverse-planning system. In the following sections, we will describe the dose calculations in the inverse-planning system and the Monte Carlo simulations. We will show the dose distributions for homogeneous and heterogeneous phantoms and discuss the effect of material density and atomic number on the final dose calculations.

2. Materials and method

2.1. Treatment planning and dose measurement

The treatment planning optimization system used in this work is the Corvus inverse-planning system. The inverse planning process employs a simulated annealing optimization algorithm (Webb 1992). The dose calculation algorithm used for the inverse planning process is a finite-size pencil beam (FSPB) algorithm, which uses predetermined beamlet dose distributions. The beamlet distributions were derived from measured dose distributions and normalized to produce consistent output factors for various field sizes. The patient inhomogeneity correction is made by 'stretching' the beamlet distribution proportionally based on the equivalent pathlength. Some details of the dose calculations have been described by Holmes *et al* (1998) and Boyer *et al* (1999). The monitor unit calculations for a 'step-and-shoot' leaf sequence algorithm have been discussed by Boyer *et al* (1999). The effect of the leaf leakage is accounted for in Corvus by reducing the original beamlet weight by the same amount as the accumulated leakage for a given leaf sequence. This method works well for those beamlets whose weights are greater than the estimated leakage. If the beamlet weights are smaller than the leakage this method will underestimate the dose as any remaining leakage effect cannot be accounted for and the initial dose calculation does not include any leaf leakage effect (which is unknown before a leaf sequence is generated for the field). The Corvus system has been commissioned for clinical IMRT treatment planning (Xing *et al* 1999) and used for treating head and neck patients with IMRT (Boyer *et al* 1998).

In order to test the Corvus system, inverse plans were computed for various target shapes placed in the centre of a cylindrical water phantom having a diameter of 30 cm. Comparisons of the Corvus dose distributions with measurements have been reported in detail by Boyer *et al* (1999). In this work, we have computed the dose distributions for these plans using Monte Carlo methods (see descriptions below). For completeness, we briefly describe the plans and the measurements below. Inverse plans were computed for different hypothetical targets with different numbers of beams directed toward the axis of the cylinder at the centre of the target and spaced at equal angles. The treatments were delivered using a dynamic multileaf collimator (Varian Oncology Systems, Palo Alto, CA). The leaf sequences computed within the Nomos software were written into files with formats conformed to the requirements of the Varian digital control software. The leaf sequences were delivered using the monitor units calculated by the Corvus system. The absolute dose delivered by the leaf sequences was measured in the 30 cm diameter cylindrical water phantom using a 0.147 cm^3 ionization chamber (Wellhöfer Dosimetrie, Schwartzenbruck, Germany) following the AAPM TG-21 protocol (AAPM 1983). No corrections were made for the variation in the chamber displacement effect, which depends on the dose gradient at the measurement point and the chamber diameter. This may introduce an up to 2% uncertainty in the measured dose for the 6 mm diameter chamber used (the dose gradient was 5–8% per centimetre at some measurement points). The chamber positioning uncertainty was about 0.1 cm. The overall uncertainty in the measured dose was estimated to be about 3% (1σ).

2.2. The Monte Carlo simulation

We have used BEAM and DOSXYZ (Rogers *et al* 1995a, b, Ma *et al* 1995) Monte Carlo codes for the accelerator head simulation and dose calculation in the patient respectively. Both codes were EGS4 (Electron Gamma Shower version 4, Nelson *et al* (1985)) user codes, running under the UNIX operating system, developed through the Omega project for Monte Carlo treatment planning dose calculations (Mackie *et al* 1994). Detailed descriptions of the software can be

found from Rogers *et al* (1995a, b). A detailed description of the clinical implementation of the Monte Carlo code system was given in a previous publication (Ma *et al* 1999).

Two types of clinical linear accelerators were simulated for the clinical implementation of Monte Carlo dose verification in this work: Varian Clinac 2100C and 2300C/D (Varian Oncology Systems, Palo Alto, CA). The dimensions and materials for the accelerator components were incorporated according to the manufacturer's specifications. Electron beams emerging from the vacuum exit window were assumed to be monoenergetic and monodirectional with a beam radius of 0.1–0.2 cm. These were found to be reasonable assumptions to achieve an acceptable dose calculation accuracy of about 2% of the dose maximum ($D_{\max}$) anywhere in the phantom for clinical radiotherapy applications (Kapur *et al* 1998, Ma 1998, Ma *et al* 1999). We obtained accurate phase-space data for photon beams with nominal energies of 4, 6 and 15 MV. The energy cut-offs for electron transport in the accelerator simulation (ECUT and AE) 700 keV (kinetic + rest mass) and for photon transport (PCUT and AP) 10 keV. The maximum fractional energy loss per electron step (ESTEPE) was 0.04. The bremsstrahlung splitting and Russian roulette options were implemented for photon beam simulations (Rogers *et al* 1995b). The ICRU recommended compositions and stopping power values were used for the materials used in the accelerator simulations (ICRU 1984). The phase-space data were scored at a plane immediately above the photon jaws. The number of particles in a photon beam file was about 50 million. Field shaping by photon jaws, blocks and the MLC was further simulated using BEAM and the phase-space data could be stored temporarily or used directly for dose calculations.

The DOSXYZ code was designed for dose calculations in a 3D rectilinear voxel (volume element) geometry (Ma *et al* 1995). Voxel dimensions were completely variable in all three directions. Every voxel could be assigned to a different material. The cross-section data for the materials used were available in a pre-processed PEGS4 cross-section data file. The mass density of the material in a DOSXYZ calculation was varied based on the patient's CT data, although the density effect corrections for the stopping powers of the material remain unchanged (Ma *et al* 1999). The voxel dimensions and materials were defined in a DOSXYZ input file together with the transport parameters such as ECUT, PCUT, ESTEPE and the parameters required by PRESTA (Bielajew and Rogers 1988). The phase-space data obtained from a BEAM simulation was used as a source input with variable source positions and beam incidence angles. Dose contributions from different beam components were selectively calculated based on the particle charge or the LATCH settings specified in the BEAM simulation. DOSXYZ produced a data file that contained geometry specifications such as the number of voxels in all three directions and their boundaries as well as the dose values and the associated (1σ) statistical uncertainties in the individual voxels.

The DOSXYZ code has been modified to read the MLC leaf sequence files for IMRT treatment. For this study, the Varian dynamic MLC leaf sequence files (G-version) generated using a step-and-shoot leaf sequencing algorithm, were used. The monitor units for each leaf sequence were integrated into a two-dimensional map (grids). The dimensions of the map at the isocentre (100 cm from the virtual point source position) are 40 cm in both the x and y directions and the grid sizes were 0.1 cm. The monitor units for the open areas were accumulated for each of the pixels, while for the closed areas a fraction of the monitor units were accumulated based on the measured MLC leakage factor for each beam energy. Thus, the integrated intensity map has included the averaged leaf leakage effect but ignored the influence of the leaf shape (tongue and groove) and the variation of the spatial and spectral distributions due to photon attenuation and scattering in the MLC leaves. This is considered to be a reasonable approach since, unless the effect of organ motion and patient set-up uncertainty has been accounted for properly, the averaged leaf leakage is a more realistic quantity than

the explicit leakage through the leaf and the tongue and groove for estimating the overall dose in a patient during the whole treatment course. The transmission factor for the areas under the photon jaws was assumed to be zero. The dimensions of the photon jaw opening were set according to the actual treatment set-ups. Further modifications were made to simulate several gantry angles in the same run. The leaf sequence files were read sequentially and the gantry angle was changed automatically after the simulation of a photon field was completed.

During the Monte Carlo simulation, the weight of a phase-space particle was altered based on the value of the pixel in the intensity map through which the particle was travelling. To improve the simulation efficiency, two variance reduction techniques were implemented in the DOSXYZ code, particle splitting and Russian roulette (Rogers and Bielajew 1990). The former was applied to the particles with weight greater than unity and the latter was applied to the particles with weight smaller than unity. The splitting and Russian roulette processes were implemented in such a way that the resulting particles would have identical weighting factors. Using uniform weighting factors will generally improve the statistical uncertainty of a simulation.

For patient dose calculations, the simulation phantom was built from the patient's CT data with up to $128 \times 128 \times 128$ voxels (uniform in any dimensions). The side of a voxel varied from 0.2 to 0.4 cm. The EGS4 transport parameters were set to ECUT = AE = 700 keV, PCUT = AP = 10 keV and ESTEPE = 0.04. The number of particle histories simulated ranged from 300 million to 1 billion for up to nine gantry angles for an IMRT treatment. The 1σ statistical uncertainty in the dose was generally 1–2% of the $D_{\max}$ value. The CPU time required for an IMRT simulation was 3–15 h on a single Pentium III 450 MHz PC depending on the beam energy and field sizes.

3. Results

3.1. Comparisons in homogeneous water phantoms

Both the inverse-planning system and the Monte Carlo dose calculation system have been commissioned for routine clinical applications (Xing *et al* 1999, Ma 1998, Ma *et al* 1999). Both systems regenerated the PDD curves and the dose profiles at various depths to within 2% of the dose maximum values of the measured beam data for various field sizes and source to surface distances (SSD). The dose distributions given by the Corvus system agreed with measurements to about 3% in a cylindrical water phantom with various hypothetical target shapes (Boyer *et al* 1999). Figure 1 shows the dose distributions in a 30 cm diameter water cylinder irradiated by seven 6 MV intensity-modulated photon beams calculated by Corvus and by the Monte Carlo simulations. The critical structure is in the centre of the water cylinder immediately next to the C-shaped target. A beamlet size of 1 cm $\times$ 1 cm was used in the optimization calculation. The leaf sequencing algorithm used 20 intensity levels. The isodose lines calculated by both systems agreed within about 4% or a shift in isodose lines within about 0.3 cm. These small discrepancies were thought to be partially due to the approximations used by Corvus in accounting for the effect of MLC leaf leakage. Considering that the average leaf leakage is about 1.5% for a 6 MV beam and the total MU required to deliver an IMRT field is about three times more than that required by a conventional field, the estimated accumulated leaf leakage beneath a completely closed leaf pair is about 4.5%. Thus, a few per cent of the observed dose difference may be attributed to the difference in leaf leakage implementation between Corvus and Monte Carlo.

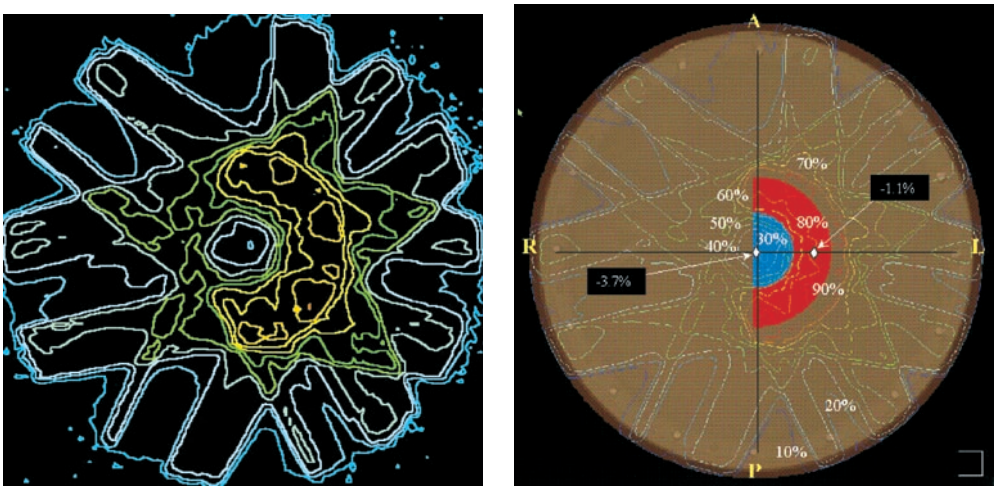

(*a*) (*b*)

Figure 1. Comparison of 6 MV photon beam (seven co-planar fields at 26, 77, 180, 231, 283 and 334° gantry angles) dose distributions in a water cylinder calculated by Monte Carlo (*a*) and Corvus (*b*). The differences between the Corvus calculations and measurements using an ion chamber are shown for certain locations (arrows).

3.2. Comparisons in CT phantoms

In this work, we have compared the dose distributions calculated by Monte Carlo and the Corvus FSPB algorithm for various treatment sites to identify potential treatment situations that may benefit from dose accuracy improvements. In the following examples, we show two typical IMRT treatment plans computed by the Corvus inverse planning system and verified by the Monte Carlo system.

3.2.1. Prostate. To explore the effect of photon and electron transport on IMRT dose calculations, we show in figure 2 an IMRT prostate treatment plan calculated by Monte Carlo simulation and the Corvus system. The plan was generated using the Corvus system for 15 MV photon beams with nine gantry angles (20, 60, 100, 140, 220, 260, 300 and 340°). The beam intensity was modulated using a Varian dynamic MLC with 80 leaves. In both calculations, the isodose lines represent the absolute dose values in the patient. It can be seen that the dose values in the target (the prostate) agreed very well between the Corvus calculations and the Monte Carlo simulations. Similar results were found for six other prostate cases compared (not shown). The difference in the average dose to the target volume was 1.6% between Monte Carlo and Corvus and the maximum dose difference in the target dose was 3.4%. This confirms that both calculation algorithms can predict dose distributions in homogeneous phantoms accurately. The dose values in the nearby critical structures also agreed to 3–7% of the prescribed target dose. For the case shown in figure 2(*c*), the maximum difference was about 3 Gy in the rectum. However, other cases also showed the maximum differences in the bladder. These differences may be considered to be clinically acceptable.

The dose values in the regions near the bony structures sometimes showed a difference of a few per cent between the Corvus and the Monte Carlo calculations. These discrepancies may be partially explained by the effect of electron backscatter from the bone (high atomic number and high density) to the soft tissue, which was accurately accounted for by the Monte Carlo

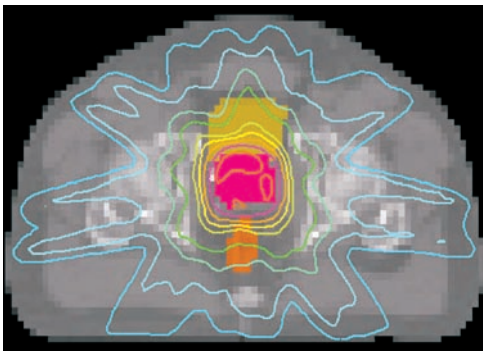

(*a*)

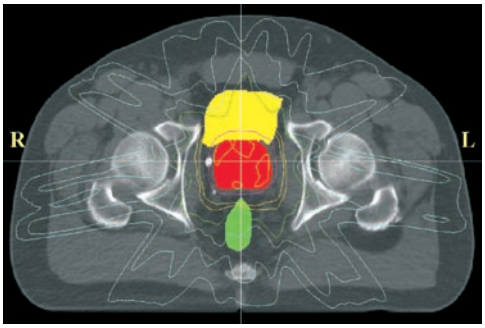

(*b*)

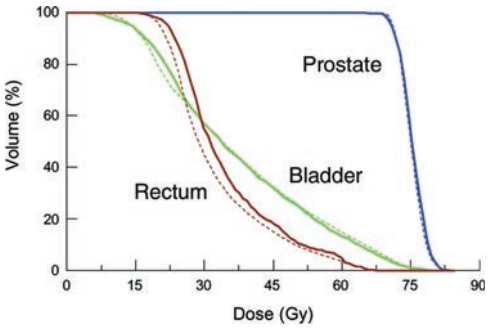

(*c*)

Figure 2. Comparison of 15 MV photon beam (nine co-planar fields) dose distributions for a prostate treatment calculated by Monte Carlo (*a*) and Corvus (*b*). The isodose lines are 77.2, 70.0, 56.1, 48.9, 35.0, 27.8, 21.1 and 13.9 Gy respectively in each figure. (*c*) The dose volume histograms as calculated by Monte Carlo (full curves) and Corvus (broken curves).

simulation but not in a FSPB algorithm. There have been several Monte Carlo studies in the literature showing similar discrepancies between the Monte Carlo algorithm and the correction based calculation algorithms in dose build-up or build-down regions near air cavities, lung and large bony structures (DeMarco *et al* 1998, Mohan 1997, Wang *et al* 1996, Ma *et al* 1999). It should be mentioned that the difference in the dose to the bone was partially due to the fact that the conventional dose calculation algorithms usually used water as the phantom material and the inhomogeneity corrections were computed using varying electron density (based on the CT numbers) while the Monte Carlo algorithm used different materials such as air, tissue, lung and bone with varying mass density calculated from the CT data. If we convert the dose to the bone material to the dose to tissue using the stopping power ratio for bone to tissue (assuming the same electron energy fluence) the dose in the bone regions will be about 3.5% higher for soft bone and about 10% higher for compact bone (ICRU 1984, Siebers *et al* 2000). We will discuss this issue further in section 4. Anyway, the dose in the surrounding tissue regions should not be affected by the conversion, which was mainly caused by the perturbation of the electron fluence by the nearby inhomogeneous anatomy.

3.2.2. Vertebra. Figure 3 shows the dose distributions for the treatment of the vertebra calculated by both Monte Carlo simulation and the Corvus system. The plan was generated using the Corvus system for 15 MV photon beams with nine co-planar gantry angles (20, 55,

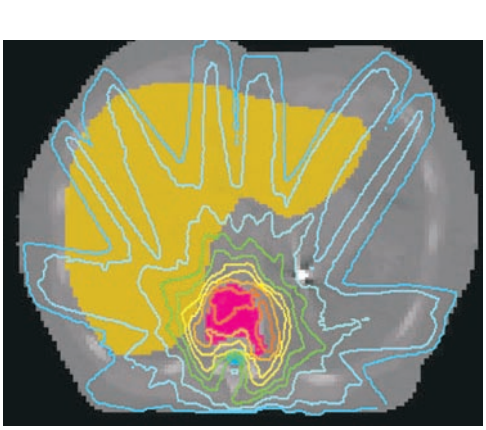

(*a*)

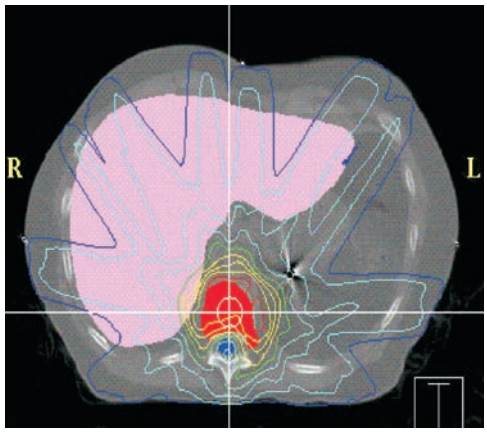

(*b*)

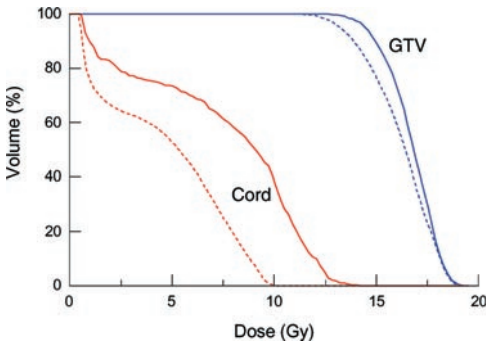

(*c*)

Figure 3. Dose distributions for the treatment of the vertebra calculated by Monte Carlo (*a*) and by Corvus (*b*) for 15 MV photons (nine co-planar fields). The isodose lines are 17.6, 15.6, 13.7, 11.7, 9.8, 7.8, 5.9, 3.9 and 2.0 Gy respectively in each figure. (*c*) The dose volume histograms as calculated by Monte Carlo (full curves) and Corvus (broken curves) for the target and the spinal cord.

90, 140, 180, 220, 260, 300 and 340°). The intensity was modulated using a Varian dynamic MLC with 80 leaves. The prescribed target dose was 18 Gy. The maximum dose in the target showed good agreement between Corvus and Monte Carlo (figure 3(*c*)). The Monte Carlo dose distribution showed slightly better target coverage than the Corvus dose distribution (a 2 Gy difference in the minimum target dose). Because the cord was sometimes immediately next to the target region the maximum cord dose was expected to be equal to or higher than the minimum target dose. This was confirmed by the Monte Carlo simulations (see figure 3(*c*)). In the regions near large bony structures (such as the cord) differences of more than 20% of the prescribed target dose could be seen between the Corvus calculation (10 Gy) and the Monte Carlo simulation (14 Gy). The difference in the dose to the cord was thought to be due in part to electron scattering from the surrounding bone, which could not be modelled properly using the FSPB algorithm. Another possible reason might be due to the implementation of the heterogeneity and leaf leakage corrections in the FSPB model. Although the photon beams were optimized to avoid the cord, electrons could reach the cord and the dose to the cord could be enhanced due to the high-density material surrounding it and/or photon leaf leakage that is not included in the dose calculation during the inverse planning process. Further studies are

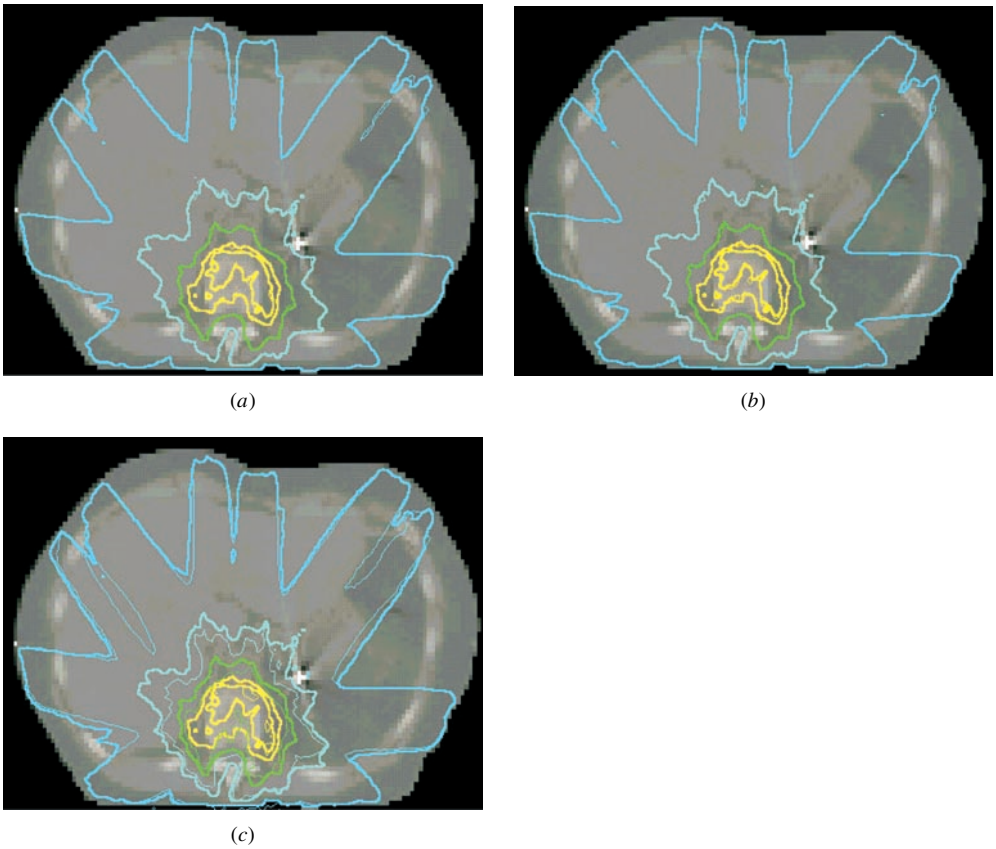

(*a*) (*b*)

(*c*)

Figure 4. Dose distributions for different tissue types and material densities: (*a*) tissue and bone with variable density (thick line) and tissue with unity density (thin line); (*b*) tissue and bone with variable density (thick line) and tissue with variable density (thin line); and (*c*) tissue and bone with variable density (thick line) and tissue with unity density and bone with 10 g cm^{-3} density (thin line). The phantom geometry and beam arrangements are the same as in figure 3. The isodose lines are given as 10, 30, 50, 70 and 80% of the prescribed target dose.

needed to understand these differences if more access to the FSPB and leaf sequence algorithms in the Corvus system is available.

4. Discussion

Several important factors may affect the Monte Carlo calculated dose distributions and the DVH curves. First, the isodose lines and the DVH curves are affected by the materials used in the patient CT phantom, i.e. whether we plot dose to tissue only or dose to any material (such as air, tissue or bone). It seems reasonable that our previous experience was based on dose to tissue (or dose to water, the difference between the two is within 1%) and therefore the dose values should be expressed as dose to tissue. However, it can also be argued that the real dose to the biological material such as bone should be given whenever possible. Only in this way can the relationship between the 'old' practice and new experience be established.

To understand the effect of the conversion of the dose to different materials, we show in figure 4 the dose distributions calculated using Monte Carlo with different materials and

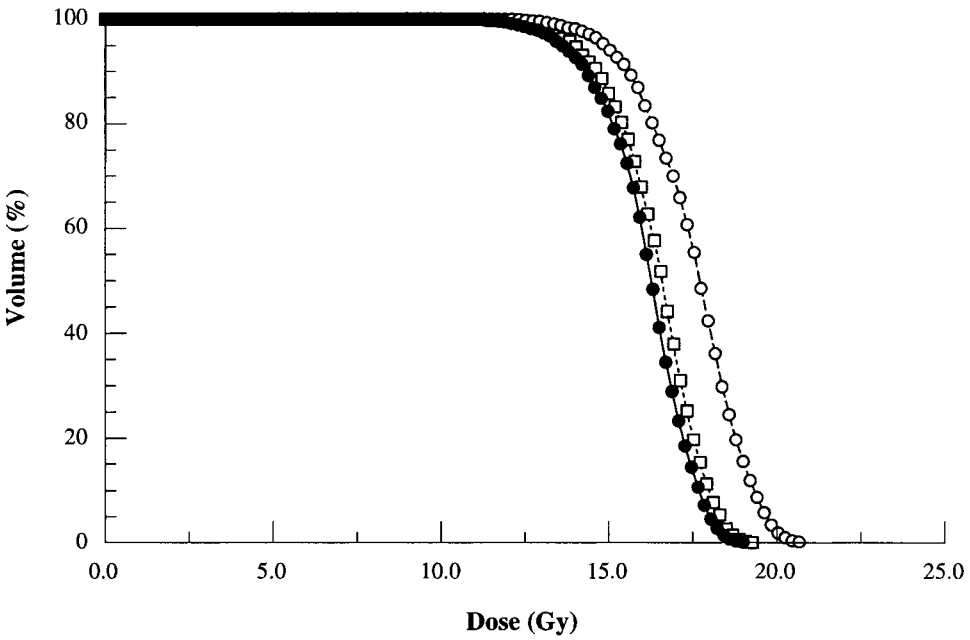

Figure 5. Dose volume histograms for the GTV in figure 3. Full circles are obtained using a CT phantom consisting of air, tissue and bone of variable density with dose calculated for each material. Open circles are obtained using the same phantom with dose converted to tissue using the stopping power ratios of tissue to bone or tissue to air. Open squares are obtained using a phantom consisting of only tissue of variable density.

density configurations for the IMRT case shown in figure 3. In figure 4(*a*), the dose distribution was calculated using tissue with unit density and air. This phantom should not show any heterogeneity effect due to the change in tissue (or bone) densities. In figure 4(*b*), the dose distribution was calculated using air and tissue with variable density converted from the CT data. This is similar to the phantom used by the Corvus system. In figure 4(*c*), the dose distribution was calculated with air, unit density tissue and 10 g cm^{-3} density bone. For comparison, the dose distribution calculated using air, tissue and bone with proper densities converted from the CT data is shown in each figure. The isodose curves were computed by normalizing the dose values to the prescribed target dose. The differences in the isodose lines in figure 4(*a*) and (*b*) are small (2–3%). This is also clearly shown in figure 5 for the target DVHs. The difference between dose to tissue and dose to bone would be about 3.5% for soft bone and about 10% for hard bone (Siebers *et al* 2000) if converted using the stopping power ratios for tissue to bone (or soft bone) at these beam qualities, assuming the same electron energy fluence. Clearly, such conversion is not equivalent to performing the Monte Carlo simulation using a water (or tissue) phantom with variable mass (or electron) density. It is known that electron backscattering from the high atomic number materials may perturb the dose in tissue near the tissue–bone interface. This effect is less significant when dose values are averaged over course scoring volumes (0.3–0.4 cm voxels). In figure 4(*c*), the density of bone was artificially increased to 10 g cm^{-3} which caused significant attenuation of the beams and therefore altered the doses behind the bones. The effects on the surface doses are smaller than for the high dose regions. The maximum dose for the artificially high-density bone geometry is about 15% lower than that for the phantom with normal material density.

Although Monte Carlo dose calculations are time-consuming it is possible to use Monte Carlo calculated dose distributions to verify the IMRT treatment plans in order to detect any cases where the FSPB dose calculation algorithm as implemented in Corvus may fail to predict the dose perturbation effect near inhomogeneities. Monte Carlo simulation may also be used directly for IMRT beamlet distribution calculation as a practical solution to this problem. Our experiences show that a factor of two to three more Monte Carlo particle histories are needed for an IMRT treatment simulation compared with a conventional photon treatment simulation to achieve the same statistical uncertainty. This is because more monitor units are needed to deliver intensity modulated photon fields; more particles will be simulated in a Monte Carlo calculation but many of them will be stopped by the MLC leaves. Therefore, the CPU time per photon history for an IMRT simulation is less than that for a conventional field. Using the existing computing power (8 CPUs) of the Corvus system, the calculation time for a typical 'inverse plan' would be increased from the current 0.5–1 h to 2–4 h with two Monte Carlo calculations. The pre-optimization dose calculation will provide the beamlet distributions for the optimization process, which take into account the effect of the accelerator head scatter and inhomogeneous anatomy of the patient. The post-optimization dose calculation will include the effects due to leaf leakage, leaf scatter and photon backscatter into the monitor chamber after the sequence of MLC leaf movement and jaw positions has been generated. Further studies are under way on a Monte Carlo dose calculation based inverse planning system (Pawlicki *et al* 1999, Ma *et al* 2000).

5. Summary

We have implemented a Monte Carlo system for routine radiotherapy treatment planning dose calculations. In our previous publications we have shown that Monte Carlo simulations agreed with measurements to within 2% for various clinical beam set-ups in homogeneous and heterogeneous phantoms. Based on these results, we have moved one step nearer to using the Monte Carlo simulations to verify the IMRT dose distributions computed by the Corvus system, which employs a FSPB algorithm for beamlet dose calculations, assuming that the Monte Carlo simulations are accurate at the 2% level for patient phantoms built from CT data.

Our results showed that the FSPB algorithm was adequate for most of the IMRT cases where the target was not immediately adjacent to the critical structures. However, the FSPB algorithm may not accurately predict the dose distributions in and near inhomogeneities in some cases. The dose in the target volume calculated by the Corvus system differed from the Monte Carlo results by more than 5%, while the dose to the critical organ differed by more than 20% of the prescribed target dose for a few cases. This suggests that, for such cases, more accurate dose calculation algorithms than that currently implemented in Corvus should be used for intensity-modulated radiotherapy treatment planning.

Acknowledgments

We would like to acknowledge Varian Oncology Systems, Palo Alto, CA, for providing detailed information on the Varian Clinac linear accelerators and Nomos Corp., Sewickley, PA, for the inverse-planning system. We would like to thank our colleagues, Sam Brain, Todd Koumrian, Behrooz Tofighrad and Michael Luxton, for help with the computers and software support. We are grateful to Dr Iwan Kawrakow for the DOSXYZ_ SHOW program to plot isodose distributions, and to Jinsheng Li and Michael Luxton for modifications to the program to display structures of interest and to compare two isodose distributions on the same plot.

This investigation was supported in part by grants CA78331 from the NIH, BC971292 from the DOD, Seed Cycle 1 from the RSNA Research and Education Fund, and a consortium agreement with the NumeriX, LLC.

References

AAPM 1983 AAPM TG-21, A protocol for the determination of absorbed dose from high-energy photons and electrons *Med. Phys.* **10** 741

Bielajew A F and Rogers D W O 1988 Variance-reduction techniques *Monte Carlo Transport of Electrons and Photons* ed T M Jenkins, W R Nelson, A Rindi, A E Nahum and D W O Rogers (New York: Plenum) pp 407–19

Boesecke R, Doll J, Bauer B, Schlegel W, Pastyr O and Lorenz M 1988 Treatment planning for conformation therapy using a multileaf collimator *Strahlenther. Onkol.* **164** 151–4

Boyer A L, Geis P B, Grant W, Kendall R and Carol M 1997 Modulated-beam conformal therapy for head and neck tumors *Int. J. Radiat. Oncol. Biol. Phys.* **39** 227–36

Boyer A L, Xing L, Ma C-M, Curran B, Hill R, Holmes T and Bleier A 1999 Theoretical consideration of monitor unit calculations for intensity modulated beam treatment planning (abstract) *Med. Phys.* **26** 187–95

Boyer A L, Xing L, Ma L and Forster K 1998 Verification and delivery of head and neck intensity modulated radiotherapy *Med. Phys.* **25** A200–1

Brahme A 1988 Optimal setting of multileaf collimators in stationary beam radiation therapy *Strahlenther. Onkol.* **164** 343–50

Brewster L, Mohan R, Mageras G, Burman C, Leibel S and Fuks Z 1995 Three dimensional conformal treatment planning with multileaf collimators *Int. J. Radiat. Oncol. Biol. Phys.* **33** 1081–89

Chui C S, LoSasso T and Spirou S 1994 Dose calculations for photon beams with intensity modulation generated by dynamic jaw or multileaf collimators *Med. Phys.* **21** 1237–43

Convery D J and Rosenbloom M E 1992 The generation of intensity-modulated fields for conformal radiotherapy by dynamic collimation *Phys. Med. Biol.* **37** 1359–74

Convery D J and Webb S 1997 Calculation of the distribution of head-scattered radiation in dynamically-collimated MLC fields *Proc. 12th Int. Conf. on the Use of Computers in Radiation Therapy (Salt Lake City, UT)* pp 350–3

Cunningham J R and Battista J J 1995 Calculation of dose distributions for x-ray therapy *Phys. Canada* **51** 190–218

DeMarco J J, Solberg T D and Smathers J B 1998 A CT-based Monte Carlo simulation tool for dosimetry planning and analysis *Med. Phys.* **25** 1–11

Fraass B A, McShan D L, Kessler M L, Matrone G M, Lewis J D and Weaver T A 1995 A computer-controlled conformal radiotherapy system. I: overview *Int. J. Radiat. Oncol. Biol. Phys.* **33** 1139–57

Holmes T M, Bleier A, Carol M, Curran B, DeNisi J, Hill R, Kania A, Lalonde R, Larson L and Sternick E 1998 The Corvus dose model revealed (abstract) *Med. Phys.* **25** 144

Holmes T M, Bleier A, Carol M, Curran B, Kania A, Lalonde R, Larson L and Sternick E 1997 The effect of MLC leakage on the calculation and delivery of intensity modulated radiotherapy (abstract) *Med. Phys.* **24** 997

Hounsell A R 1998 Monitor chamber backscatter for intensity modulated radiation therapy using multileaf collimators *Phys. Med. Biol.* **43** 445–54

ICRU 1984 Radiation dosimetry: stopping powers for electrons and positrons *ICRU Report 37* (Bethesda, MD: ICRU)

Kapur A, Ma C-M, Mok E and Findley D 1997 Characterization of small field electron beams for radiotherapy using Monte Carlo simulations *Proc. 12th Int. Conf. on the Use of Computers in Radiation Therapy (Salt Lake City, UT)* pp 157–8

Kapur A, Ma C-M, Mok E, Findley D and Boyer A L 1998 Monte Carlo calculations of clinical electron beam output factors *Phys. Med. Biol.* **43** 3479–94

Kutcher G J, Mageras G S and Leibel S A 1995 Control, correction and modeling of set-up errors and organ motion *Semin. Radiat. Oncol.* **5** 134–45

Leibel S A, Kutcher G J and Mohan R *et al* 1992 Three-dimensional conformal radiation therapy at the Memorial Sloan-Kettering Cancer Center *Semin. Radiat. Oncol.* **2** 274–89

Ling C C *et al* 1996 Conformal radiation treatment of prostate cancer using inversely-planned intensity-modulated photon beams produced with dynamic multileaf collimation *Int. J. Radiat. Oncol. Biol. Phys.* **35** 730–41

LoSasso T, Chui C S, Kutcher G J, Leibel S A, Fuks Z and Ling C C 1993 The use of multileaf collimators for conformal radiotherapy of carcinomas of the prostate and nasopharynx *Int. J. Radiat. Oncol. Biol. Phys.* **25** 161–70

Ma C-M 1998 Characterization of computer simulated radiotherapy beams for Monte Carlo treatment planning *Radiat. Phys. Chem.* **53** 329–44

Ma C-M, Mok E, Kapur A and Findley D 1997 Improvement of small-field electron beam dosimetry by Monte Carlo simulations *Proc. 12th Int. Conf. on the Use of Computers in Radiation Therapy (Salt Lake City, UT)* pp 159–62

Ma C-M, Mok E, Kapur A, Pawlicki T A, Findley D, Brain S, Forster K and Boyer A L 1999 Clinical implementation of a Monte Carlo treatment planning system for radiotherapy *Med. Phys.* **26** 2133–43

Ma C-M, Pawlicki P, Lee M C, Jiang S B, Li J S, Deng J, Yi B, Mok E and Boyer A L 2000 Energy- and intensity-modulated electron beams for radiotherapy *Phys. Med. Biol.* **45** 2293–311

Ma C-M, Reckwerd P, Holmes M, Rogers D W O and Geiser B 1995 DOSXYZ users manual *National Research Council Report* PIRS-0509(B) (Ottawa: NCRC)

Mackie T R, Holmes T W, Reckwerdt P J and Yang J 1995 Tomotherapy: optimized planning and delivery of radiation therapy *Int. J. Imaging Syst. Technol.* **6** 43–55

Mackie T R, Reckwerdt P, McNutt T, Gehring M and Sanders C 1996 Photon beam dose calculations *Teletherapy: Present and Future* ed T R Mackie and J R Palta (Madison, WI: Advanced Medical Publishing) pp 103–35

Mackie T R, Reckwerdt P and Papanikolaou N 1995 3-D photon beam algorithms *3-D Radiation Treatment Planning and Conformal Therapy* ed J A Purdy and B Emami (Madison, WI: Medical Physics Publishing) pp 201–22

Mackie T R *et al* 1994 The OMEGA project: comparison among EGS4 electron beam simulation, 3D Fermi–eyges calculations and dose measurements *Proc. 11th Int. Conf. on the Use of Computers in Radiation Therapy (Manchester, UK)* pp 152–3

Mageras G S *et al* 1994 Initial clinical experience with computer-controlled conformal radiotherapy using the MM50 microtron *Int. J. Radiat. Oncol. Biol. Phys.* **30** 971–8

McShan D L, Fraass B A, Kessler M L, Matrone G M, Lewis J D and Weaver T A 1995 A computer-controlled conformal radiotherapy system. II: sequence processor *Int. J. Radiat. Oncol. Biol. Phys.* **33** 1159–72

Mohan R 1997 Why Monte Carlo? *Proc. 12th Int. Conf. on the Use of Computers in Radiation Therapy (Salt Lake City, UT)* pp 16–18

Nelson R, Hirayama H and Rogers D W O 1985 The EGS4 code system *Stanford Linear Accelerator Center Report* SLAC-265 (Stanford, CA: SLAC)

Oldham M and Webb S 1997 Intensity-modulated radiotherapy by means of static tomotherapy: a planning and verification study *Med. Phys.* **24** 827–36

Pawlicki T A, Jiang S B, Deng J, Li J S and Ma C-M 1999 Monte Carlo calculated beamlets for photon beam inverse planning (abstract) *Med. Phys.* **26** 1064–5

Powlis W D, Smith A, Cheng E *et al* 1993 Initiation of multileaf collimator conformal radiation therapy *Int. J. Radiat. Oncol. Biol. Phys.* **25** 171–9

Rogers D W O and Bielajew A F 1990 Monte Carlo techniques of electrons and photons for radiation dosimetry *Dosimetry of Ionizing Radiation* vol 3, ed K Kase, B E Bjarngard and F H Attix (New York: Academic) pp 427–539

Rogers D W O, Faddegon B A, Ding G X, Ma C M, Wei J S and Mackie T R 1995a BEAM: a Monte Carlo code to simulate radiotherapy treatment units *Med. Phys.* **22** 503–25

Rogers D W O, Ma C M, Ding G X and Walters B 1995b BEAM users manual *National Research Council Report* PIRS-0509(A) (Ottawa: NRC)

Siebers J V, Keall P J, Nahum A E and Mohan R 2000 Converting absorbed dose to medium to absorbed dose to water for Monte Carlo based photon beam dose calculations *Phys. Med. Biol.* **45** 983–95

Wang L, Chui C and Lovelock M 1998 A patient-specific Monte Carlo dose-calculation method for photon beams *Med. Phys.* **25** 867–78

Wang X, Spirou S, LoSasso T, Stein J, Chui C and Mohan R 1996 Dosimetric verification of intensity modulated fields *Med. Phys.* **23** 317–28

Wong J W and Purdy J A 1990 On the methods of inhomogeneity corrections for photon transport *Med. Phys.* **17** 807–14

Webb S 1992 Optimization by simulated annealing of three-dimensional conformal treatment planning for radiation fields defined by multi-leaf collimator: II. Inclusion of two-dimensional modulation of x-ray intensity *Phys. Med. Biol.* **37** 1689–704

——1997 *The Physics of Conformal Radiotherapy: Advances in Technology* (Bristol: Institute of Physics Publishing)

Xing L, Curran B, Hill R, Holmes T, Ma L, Forster K and Boyer A L 1999 Dosimetric verification of a commercial inverse treatment planning system *Phys. Med. Biol.* **44** 463–78

Yu C X, Symons J M, Du M N, Martinez A A and Wong J W 1995 A method for implementing dynamic photon beam intensity modulation using independent jaws and multileaf collimators *Phys. Med. Biol.* **40** 769–87